Welding in the World (2023) 67:1325–1336
https://doi.org/10.1007/s40194-022-01460-9

RESEARCH PAPER

Wide gap brazing of NIMONIC 105 superalloy using BNi-2 filler and the effect of post braze heat treatment on joint properties

Reza Barazandeh[1] · Mohammad Ammar Mofid[1] · Mostafa Jafarzadegan[2] · Hadi Nasiri Vatan[1]

Received: 19 July 2022 / Accepted: 27 December 2022 / Published online: 28 January 2023
© International Institute of Welding 2023

Abstract

Wide gap brazing is a critical, cost-effective, and widely used technique for repairing superalloy components. However, even with careful control of the braze filler and brazing variables, formation of intermetallic phases cannot be completely avoided. In this work, wide gap brazing of NIMONIC 105 superalloy was performed in a vacuum chamber using BNi-2 alloy as filler at two different brazing temperatures of 1050 °C and 1170 °C. Then, the innovative approach of post braze heat treatment (PBHT) of diffusion-brazed bonds performed at 1000 °C to improve the joints' microstructural characteristics and mechanical properties. The phases formed in the diffusion-affected zone (DAZ), isothermally solidified zone (ISZ), and athermally solidified zone (ASZ) were comparatively studied. The investigation confirms PBHT led to a more uniform hardness profile across the joint and a more homogenous interface region via dissolution of intermetallic phases that, in turn, increases the resistance to oxidation. The shear strength of joints made at brazing temperature of 1170 °C remarkably increased from 40 to 83.8 MPa and finally reached the maximum value of 92.2 MPa via PBHT. The ductility of this specimen was as high as 19.0%, which is approximately 75% of the ductility of the base metal.

Keywords Wide gap brazing · NIMONIC 105 · Superalloy · Post braze heat treatment · Microstructure · Shear strength

1 Introduction

Nickel superalloys are known to have excellent corrosion resistance for high-temperature applications. NIMONIC alloy 105 (W. Nr. 2.4634) is a wrought nickel–cobalt-chromium-based alloy strengthened by molybdenum, aluminum, and titanium additions. It has been developed for service up to 950 °C and combines the high strength of the age-hardening nickel-based alloys with good creep resistance. The alloy is used for turbine blades, discs, forgings, ring sections, bolts, and fasteners [1]. However, the high cost of processing and fabrication of nickel superalloy components has limited their use so far. Thus, the problem of repairing the components must be faced [2]. Cost efficiency has biased the industry toward repairing as the best solution instead of replacing the component with a new one. Various attempts have been made to join nickel-based superalloys [3–6]. Fusion welding repair processes would result in inconvenient microstructural changes to the joint region, hence was not a suitable approach [7]. Braze repair is a proven approach for reliable, cost-effective life extension of gas turbine components [8, 9]. Wide gap brazing (WGB) is an efficient approach that has found a unique position in joining superalloys and repairing superalloy parts in recent years [10]. Conventional brazing, or narrow gap brazing, relies on capillary attraction, and as such, the joint gaps are limited. Since boron (B) and silicon (Si) are often used as melting point depressants in the nickel- and cobalt-based braze alloys, a small clearance of 50–100 µm is required to prevent the formation of brittle intermetallic phases in the form of borides and silicides [8]. The process is conducted in a vacuum chamber or inert atmosphere. A wide gap is considered to be larger than 500 µm, and during brazing, base metals and the braze filler are held at the brazing temperature for a short time to ensure wetting of faying surfaces

Recommended for publication by Commission XVII - Brazing, Soldering and Diffusion Bonding

✉ Mohammad Ammar Mofid
moh.ammar_mofid@iauctb.ac.ir

[1] Department of Petroleum, Mining and Material Engineering, Faculty of Civil and Earth Resources Engineering, Central Tehran Branch, Islamic Azad University, Tehran, Iran

[2] Faculty of Engineering, Imam Khomeini International University (IKIU), Qazvin 3414896818, Iran

with the braze filler melt. The specimen is then cooled from the brazing temperature, during which the braze alloy solidifies. Since the cooling occurs under non-equilibrium conditions, solidification products contain eutectic and intermetallic phases. Even with careful control of the braze filler and brazing variables, the formation of intermetallic phases cannot be wholly avoided [8]. Hadibeyk et al. declared that at low temperatures, isothermal solidification could not be completed, and a eutectic structure was formed in the bonding zone, while at high temperatures, the hindering effect of substrate elements prevented the completion of isothermal solidification [11]. Khakian et al. concluded that because of incomplete isothermal solidification, the remained liquid transforms to gamma-eutectic, and subsequently, Cr-rich boride and Ni-rich boride will form in the interface of dissimilar IN738LC and NIMONIC 75 joint [6].

The BNi filler metals commonly are used on stainless steels for oxidation resistance at temperatures up to 980 to 1095 °C [2]. BNi-2 braze alloys that contain boron and silicon as melting point depressants are the most common fillers for brazing Ni superalloys. However, the problem is that this filler develops a brittle eutectic constituent that is the source for crack initiation and propagation [12, 13]. Up to now, two approaches have been proposed to overcome these problems. In the first approach, composite fillers, which are prepared by introducing tiny ceramic particles or fibers into traditional active brazing fillers, have been employed to retard atomic diffusion and control the formation of brittle intermetallics [14]. Much research has been devoted to overcoming or at least moderating the unfavorable impact of such brittle phases by introducing silicon nanoparticles, graphene, ZrO_2 nanoparticles, TiO_2 nanoparticles, and tungsten powder into the brazing filler [14–16]. García et al. used silicon nanoparticles and claimed that this addition diminished the eutectic structure's size and promoted a uniform distribution in the bonding area [15]. Shen et al. added ZrO_2 nanoparticles into an Sn-Ag filler and showed that this addition controlled the formation of intermetallic particles during solidification [16]. Liu et al. concluded that adding graphene significantly improved the shear strength of the GH99 superalloy brazed joints. They claimed that graphene effectively retarded atomic diffusion and controlled the formation of brittle boride precipitates [14].

Another approach to overcoming or at least moderating the unfavorable impact of such eutectic and intermetallic phases is applying subsequent homogenization treatment to the diffusion-brazed bonds. Post braze heat treating (PBHT) can help to achieve a more uniform microstructure that, in turn, can minimize stress concentration in the interface and lead to stress release. As mentioned earlier, the phases formed in the centerline eutectic are deleterious to the mechanical properties. The centerline eutectic phases are avoided by completing isothermal solidification. Thought, if isothermal solidification is incomplete, the microstructure can be improved with a diffusion heat treatment [17]. According to the literature, diffusion brazing can be divided into three separate stages, including base metal dissolution, isothermal solidification, and bond region homogenization. Duvall et al. [17] have stated that isothermal solidification has a critical influence on the joint quality of the brazed joints. Pouranvari et al. stated that if isothermal solidification is completed, there would be no trace of detrimental eutectic constituents along the joint centerline. A joint almost identical to the base metal in terms of microstructure and mechanical properties can be achieved by applying subsequent homogenization treatment to the diffusion-brazed bonds [18]. However, applying PBHT to NIMONIC 105 diffusion-brazed bonds to improve the microstructural characteristics and comparison of obtained mechanical properties has not been reported.

In this study, wide gap brazing of NIMONIC 105 superalloy was performed in a vacuum chamber using BNi-2 alloy as filler at two different brazing temperatures, and then, PBHT of the specimens was performed in an inert atmosphere for two different times. Microstructural evolution, microhardness, and shear strength points of view were compared. Some remarkable results were obtained through applying PBHT. The formation of intermetallic phases was investigated by hardness test and scanning electron microscope (SEM)-energy-dispersive X-ray spectroscopy (EDS) analysis. The novelty of this study is the investigation of the influence of bonding temperature and homogenization heat treatment on the microstructure and mechanical properties of diffusion-brazed NIMONIC 105 superalloy using a BNi-2 interlayer. This innovative method is hoped to help arrive at a practical solution to applications concerning difficult to weld superalloys which are prone to the formation of deleterious intermetallic compounds.

2 Experimental procedure

NIMONIC 105 superalloy and commercially obtained BNi-2 filler were received as the experimental materials in this study. The compositions of the base metal and BNi-2 filler were analyzed experimentally. The result is listed in Table 1. BNi-2 contains boron and silicon as melting point depressants. According to ASM International, BNi-2 filler is an appropriate brazing filler metal for high-temperature, high-stress moving engine components and heavy, non-moving structures (variable gaps). It is appropriate for jet engine diffuser components [2]. Two specimens have been prepared by cutting for metallography and shear strength test with the dimensions of 20 mm × 20 mm × 2.5 mm and 40 mm × 20 mm × 2.5 mm, respectively. Figure 1 demonstrates the sample specimens as well as the experimental

Table 1 Chemical compositions of NIMONIC 105 superalloy and BNi-2 filler (wt.%)

	Ni	Co	Cr	Mo	Al	Si	Fe	Ti	Cu	B	C
NIMONIC 105 superalloy	Bal	18.41	14.93	5.01	4.64	0.11	1.0	1.37	0.2	-	0.15
BNi-2 filler	Bal	-	7.0	-	-	4.5	3.0	-	-	3.0	0.06

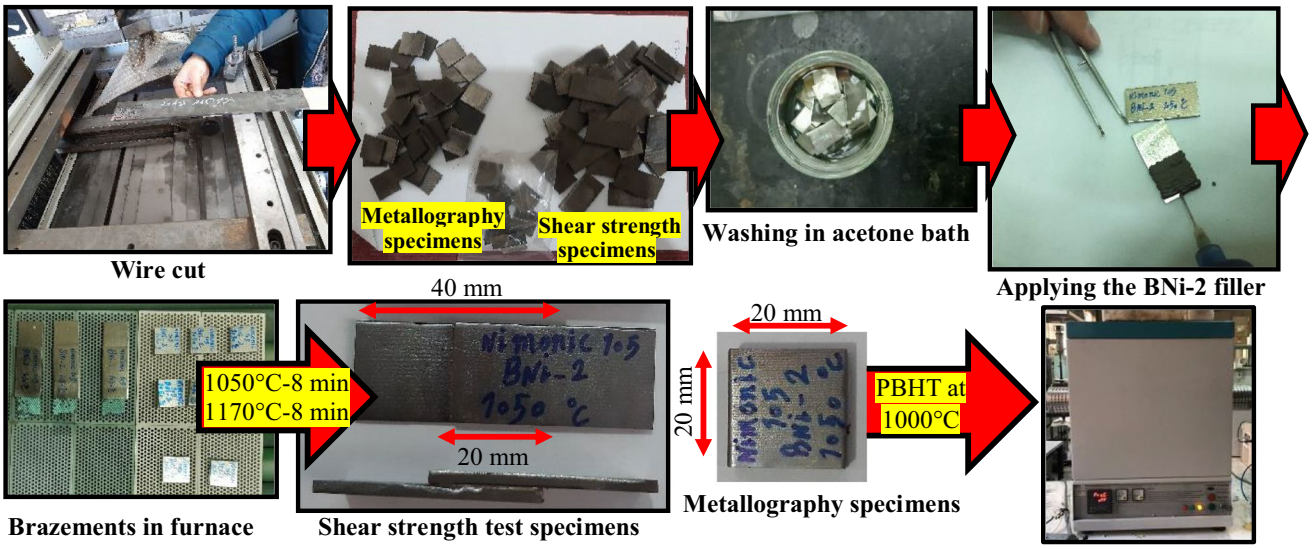

Fig. 1 Dimensions of the base metals, metallography, and shear strength test specimens and the experimental setup for diffusion brazing

setup. The specimens were ultrasonically cleaned in an acetone bath to remove adhered contaminants and then dried in air. For preparing the shear strength test specimens, the samples were cut into dimensions of 40 × 20 × 2.5 mm. Then, the BNi-2 filler in the form of paste with a thickness of 1 mm was applied to join NIMONIC 105 superalloy. Solidus and liquidus temperatures of the brazing filler are 970 °C and 1000 °C, respectively. So, brazing temperature was selected at temperatures above 970 °C. Experiments were performed in an electrical furnace with a vacuum of 1×10^{-4} Pa. The sample assembly was first heated to 750 °C and held for 30 min. Then, the temperature was increased to 950 °C and held for 30 min. Finally, the temperature was increased to a specified brazing temperature (1050 °C and 1170 °C). The holding time was 8 min. In order to investigate the effect of PBHT on microstructure and mechanical properties of the joints, homogenization of the specimens was performed at 1000 °C for 1 h and 4 h. The assemblies were cooled in the processing chamber under a vacuum.

Following brazing and PBHT, transverse cross sections were prepared for microstructural observations with an optical microscope (OM) and scanning electron microscope (SEM). The etchant is composed of a "15 ml HCl, 10 ml HNO_3, 10 ml acetic acid, and 5 ml glycerol" solution. The etching time was 5 s. SEM (TESCAN MIRA3) equipped with energy-dispersive spectroscopy (EDS) analysis system was employed to analyze the chemical composition of the present phases at the interface. For the microhardness test, a WOLPERT machine was used that was able to measure microhardness at a microscale with 50 gf load weight according to ASTM standard E384 (2017). The indenter was the diamond-based pyramid. The room-temperature shear strength of the joints was measured by a tensile test machine (INSTRON-5500R) according to ASTM standard D1002-99 at a crosshead speed of 1 mm/min.

The cyclic oxidation test was carried out in an automatic test bed designed and built for this purpose. Cyclic conditions in this device are provided through the reciprocating movement of the samples in the vertical direction into the furnace. Test samples in the form of rectangular cubes with dimensions of 12 × 7 × 2 mm were prepared according to the standard from the available raw materials, which were mainly the roots of the blades, by wire-cut method [19]. Six samples were prepared and used in the cyclic oxidation test. Considering that the surface of the samples became completely dark due to wire cutting, these oxides and other surface contaminants were removed through mechanical polishing with sandpaper no. 180, 500, and 1000, and all the corners and sharp edges of the samples were also polished. The initial weight of the samples was determined and recorded with the help of a digital scale with an accuracy of

0.0001 g after partial sanding into round shape and acetone washing of the samples.

The test consisted of 1-h cycles at 1100 °C, the details of which are as follows:

- Step 1: Place the weighed samples in special places on the sample stand.
- Step 2: Heating the furnace thermal chamber to 1100 °C.
- Step 3: As soon as the temperature reaches 1100 °C, the arm of the samples starts moving upwards, and within 5 s, the samples are placed in the center of the thermal zone.
- Step 4: Keeping the samples at 1100 °C for 1 h.
- Step 5: Moving the sample arm down and leaving the thermal chamber and the sample temperature reaching 300 °C.

Steps 1 to 5 in this experiment were repeated for 50 cycles.

In between the cycles where the weighing of the samples is not considered, the system is allowed to repeat steps 1 to 5, but if it is necessary to weigh the samples, they are removed from their place in the device and then cooled down to the temperature of the weighing environment. Following the weighing process, the samples are returned to the test cycle.

3 Results and discussion

3.1 Microstructural characterization of the joints

3.1.1 As-brazed specimens

From the Arrhenius formula, temperature is the most important parameter in any diffusion bonding process [20, 21]. Therefore, the macroscopic images and macrostructures of the joints made at 1050 and 1170 °C were studied. Figure 2 shows a typical overview of joint regions. It is obvious from Fig. 2 that with the rise of brazing temperature from 1050 (Fig. 2a) to 1170 °C (Fig. 2b), the thicknesses of dissolution and widening zones increase significantly from 470 to 850 µm, respectively. The reason is that atomic diffusion occurs evenly and thoroughly at a higher temperature. This leads to the better dissolution of the base metal in the joint area, leading to the wider joint region [22]. On the other hand, the increasing temperature raises the base metal grain size, which in turn deteriorates the mechanical properties of the base metal.

In order to better characterize the joint interface, higher magnification OM images of the zone were taken and are shown in Fig. 3. As can be seen, in addition to NIMONIC base metal (BM), three zones are recognizable: (i) the diffusion-affected zone (DAZ), (ii) the isothermally solidified zone (ISZ), and (iii) athermally solidified zone (ASZ). According to the literature [6] in DAZ, the base metal interacts with the melting point depressant (MPD) elements diffused from the filler metal, such as boron and silicon. It is apparent in Fig. 3 that the DAZ consists of globular/cuboidal and needle-like precipitates distributed in the interface. Figure 3 suggests that the morphology and distribution of these secondary phases depend on the brazing temperature.

Regarding Fig. 3, brazing temperature increment will increase the width of this DAZ from 12 (Fig. 3a) to 35 µm (Fig. 3b). On the other hand, it is apparent from Fig. 3a that the morphology of these precipitates changes from globular to needle-like, with getting away from the interface. This is in accordance with the study of Li and Liu [4, 5], who reported that the morphology of these secondary phases depends on shrinkage stresses arising from isothermal

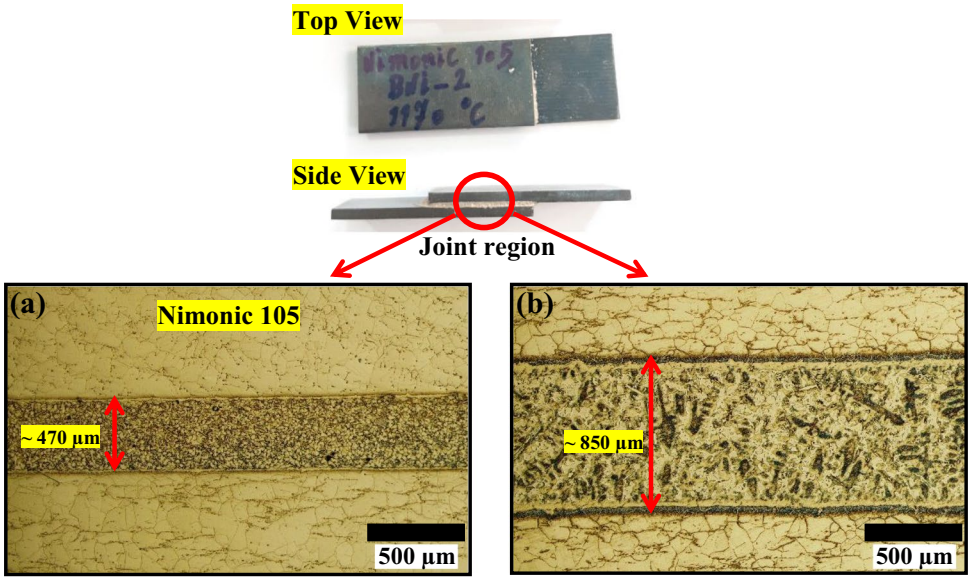

Fig. 2 Joint overview and macroscopic images of joints brazed at the time of 8 min and bonding temperature of (**a**) 1050 °C and (**b**) 1170 °C

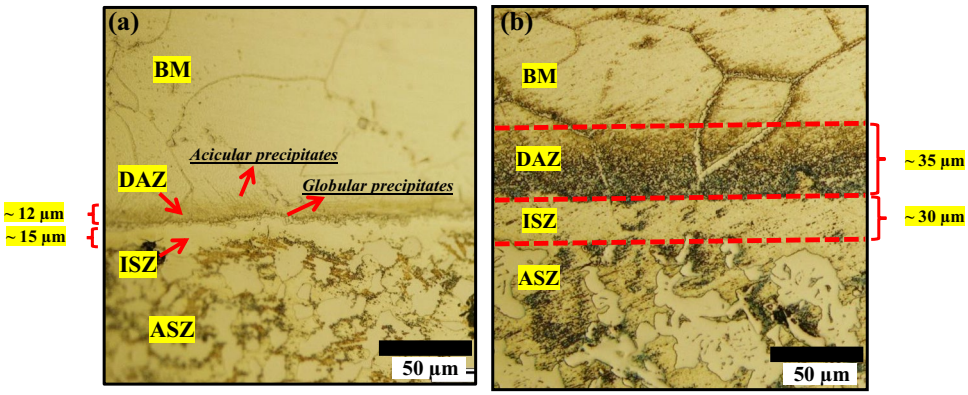

Fig. 3 Optical microscope images of the joint region for the specimens brazed at bonding temperature of **a** 1050 °C and **b** 1170 °C

solidification. At the vicinity of NIMONIC/filler interface, more shrinkage stresses developed. As a result, precipitates become spherical adjacent to this interface and acicular beyond it. Nucleation of these phases occurs at the first stages of brazing in NIMONIC 105 superalloy in short times, and as Fig. 3b shows, they will dissolve at higher temperatures.

The precipitation-free zone in Fig. 3a and b is relevant to ISZ, which is formed near NIMONIC 105/braze alloy interface. During the isothermal solidification stage, the Ni-rich gamma phase formed with solid solution strengthener, including boron and silicon, which solidifies inward. At brazing temperature, filler melts and wets the joint faying surfaces. Because of the establishment of perfect contact between solid and liquid, NIMONIC 105 begins to dissolute. At this time, MPD diffusion from filler to NIMONIC and diffusion of alloying elements from NIMONIC to filler occur. The result is an extension of liquid formation. The volume of liquid continues to increase up to the establishment of local equilibrium between solid and liquid. Once the molten filler reaches brazing temperature, the dissolution stage ceases, and at this time, isothermal solidification commences from the liquid/solid interface inward to the joint centerline. According to the microstructure shown in Fig. 3, it can be concluded that after the completion of isothermal solidification, there would be a single phase with a uniform microstructure in the bond line. The reason is that the liquid/solid interface does not experience any super cooling during isothermal solidification. Therewith, non-equilibrium segregation of solute elements is resolvable, and no secondary phases can form. Therefore, in correspondence with the literature, ISZ microstructure is a solid solution single phase [23, 24].

If insufficient time is given, isothermal solidification is unable to be complete, and the residual liquid is rejected to the center of the joint [4]. The liquid in the center becomes enriched in melting point depressants, shifting the concentration to a eutectic composition resulting in eutectic-like solidification referred to as the ASZ, as shown in Fig. 3. It is known that ISZ thickness is controlled by MPD element diffusion [6]. According to the microstructural studies in Fig. 3, it can be concluded that with the rise of brazing temperature from 1050 (Fig. 3a) to 1170 °C (Fig. 3b), the thicknesses of ISZ increase significantly from 15 to 30 µm, respectively. The reason is that the rate of MPD diffusion into base metal is higher at a higher temperature.

In order to acquire a more precise investigation of microstructural evolutions at the interface, backscattered electron (BSE) micrograph of the interface and concentration profile of some important elements (Cr, Fe, and Si) across the bonding region were taken and are shown in Fig. 4. The EDS technique is applied to identify each phase individually. Regions in a joint created at a brazing temperature of 1050 °C have been analyzed using EDS at some selected regions marked as 1, 2, and 3 in Fig. 4. The concentration of Ni, Co, Cr, Mo, Al, Si, Fe, Ti, and Cu in the aforementioned regions analyzed by EDS is listed in Table 2. Based on the compositional analysis, regions 1 and 2 (acicular and cuboidal precipitates in DAZ) contain higher chromium content in comparison with BNi-2 filler. On the other hand, boron

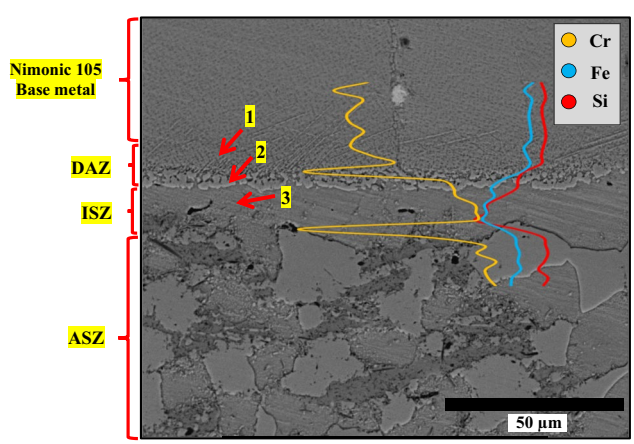

Fig. 4 BSE micrograph of the interface and concentration profile of some important elements across the bonding region for the specimens brazed at a bonding temperature of 1050 °C

solubility in nickel is very low (0.3 at.% at a temperature range of 1060 to 1120 °C [25]). As a result, when the concentration of boron exceeds from solubility limit in the base metal, secondary precipitates can form. Boron combines with chromium or molybdenum to form chromium borides within the gamma-grain boundaries. The precipitates in the DAZ were mainly composed of Ni–Cr-Mo-rich borides. This is in agreement with the results of Wu et al. [9]. During the brazing process, silicon and boron atoms diffused to the base metal from molten filler. Here (in DAZ), boron reacted with elements from base metal to form Ni–Cr-Mo-rich borides.

From Table 2, it can be found that the nickel content in the ISZ (region 3) was higher (74.45 at.%), followed by silicon (10.11 at.%) and chromium (6.37 at.%). Based on the Ni–Cr binary phase diagram, the ISZ mainly consisted of a gamma solid solution [25]. At the first stage of brazing, when the temperature of the chamber reached the melting point of the filler, BNi-2 melted gradually, and the liquid phase formed. Then, the liquid phase infiltrated into the NIMONIC 105 superalloy substrate, and boron and silicon atoms diffused to the NIMONIC 105 substrate. During the isothermal solidification stage, the diffusion process of atoms was accelerated. Boron and silicon atoms further diffused to NIMONIC substrate, and high-melting elements chromium and molybdenum of base metal dissolved and diffused into the molten filler at the same time. The presence of Ni_3(Si, B) reported in the literature [10] is in good agreement with the results of this study. This phase formed with the other elements in solid solution. The EDS line scan of elements perpendicular to the interface (Fig. 4) shows a severe decrease in chromium profile and a significant increase in silicon and iron inside the ISZ. Fe and Ni can dissolve each other infinitely during bonding. Therefore, a large number of Fe atoms can diffuse and traverse the interlayer, leading to increased Fe content (5.06 at.%) at region 3. The issue surrounding boron as an MPD is its tendency to form borides. Chromium boride often forms, which reduces the chromium content in the braze and decreases corrosion resistance. The formation of mentioned chromium boride precipitates is responsible for localized depletion in the concentration of Cr and some other refractory elements such as Mo in ISZ. These phases reduce the chromium and molybdenum concentrations from the gamma-matrix. They would have a detrimental effect on the high-temperature performance and make these regions prone to selective corrosion or oxidation. According to Table 2 in region 3 (ISZ), the main constituent is nickel (74.45 at.%) which suggests that the matrix is gamma-nickel with solid solution strengthening elements chromium (6.37 at.%), cobalt (1.29 at.%), and silicon (10.11 at.%). Analyses of region 3 showed that elements like Co, Al, and Ti, which were not present in the initial chemical composition of filler, have diffused into the joint zone. This fact confirms the transportation of solute elements into the liquid phase during the brazing and the occurrence of solid state diffusion.

The BSE micrograph of the ASZ for the sample brazed at 1170 °C is shown in Fig. 5. The formation of the eutectic that contains fine precipitates is visible in the figure. The presence of some eutectic islands and intermetallics at the centerline of the joint suggests that the isothermal solidification of the liquid phase was not completed in 8 min. As a result, the remained liquid undergoes supercooling. Under such circumstances, microstructural evolution is driven by the dissolution and diffusion of the base metal alloying elements into the joint [18]. Due to the low solubility of boron in nickel (0.3 at.% [25]), extra boron will be rejected into the molten metal.

Table 2 indicates that the ASZ in Fig. 5 contains the matrix solid solution of gamma-nickel (region 4 in Fig. 5), Ni-rich boride (region 5), and two Cr-rich phases (regions 6, 7). Gamma solid solution (region 4) is the first phase that forms and grows during cooling. Since there is a large amount of silicon (6.08 at.%), the phase that forms with the other elements in the solid solution is most likely Ni_3(Si, B). There was a significant amount of aluminum in region 5, which would most likely contribute to the gamma-prime precipitation. The ongoing formation of gamma-nickel and Ni-rich gamma-prime dendrites leads to the rejection of alloying elements such as Cr, Mo, Al, and B to liquid [26]. As a result, the remained liquid will become enriched by these elements. Phases 6 and 7 in Fig. 5 are Cr-rich boride and Cr-rich intermetallic compounds, respectively. These intermetallics would not be ideal phases to form because that would mean that chromium is being depleted from the

Table 2 EDS analysis (wt.%) of selected regions shown in Figs. 4 and 5

Region	Ni	Co	Cr	Mo	Al	Si	Fe	Ti	Cu	Possible phases
1	45.85	16.22	19.76	2.10	8.53	0.95	2.01	1.24	0.60	Ni–Cr-Mo-rich borides
2	70.33	7.40	8.64	0.83	5.77	1.98	2.23	1.34	0.58	Ni–Cr-Mo-rich borides
3	74.45	1.29	6.37	0.01	1.28	10.11	5.06	0.60	0.84	Gamma-nickel solid solution
4	69.32	6.11	7.68	0.15	4.97	6.08	3.51	0.80	0.75	Gamma solid solution
5	76.19	6.73	4.83	0.11	4.38	0.76	2.00	2.54	0.93	Ni-rich boride
6	13.57	4.96	64.18	10.22	0.95	1.48	2.88	0.83	0.66	Cr-rich boride
7	3.66	0.87	83.91	6.52	0.66	1.21	1.29	0.80	0.30	Cr-rich intermetallic compound

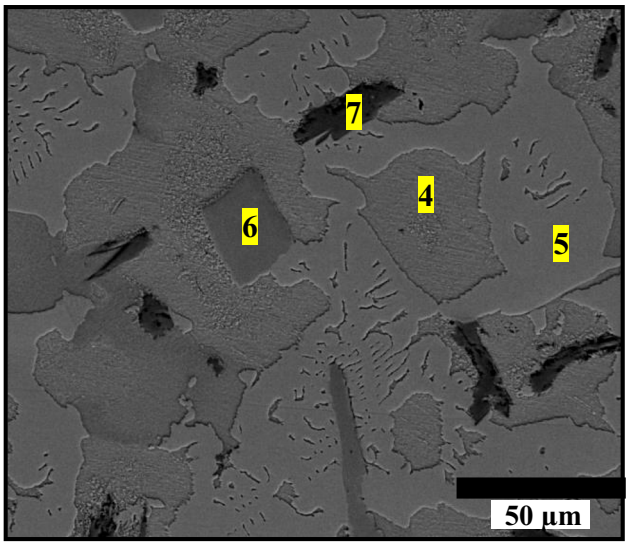

Fig. 5 BSE micrograph of the ASZ for the sample brazed at a bonding temperature of 1170 °C

matrix, thereby decreasing the corrosion resistance of the material. Arhami et al. [3] have also reported the formation of the same phases in the ASZ of diffusion-brazed IN-939 using a Ni–Cr-B interlayer.

An issue with the specimen brazed at 1170 °C was the large amount of void-like defects observed in the BSE micrograph that formed within the joint in ASZ adjacent to the Cr-rich phases (Fig. 6a). In order to determine whether these features are real voids or not, secondary electron (SE) micrograph of the same zone was taken and is shown in Fig. 6b. It is apparent from the SE image that electron number effects make the edges of surface voids brighter than the rest of the surface. It can be concluded that Fig. 6 shows many voids in ASZ, indicating a brittle braze owing to intermetallics. This agrees with the results of Kim et al. [10]. The voids formed due to solidification shrinkage in ASZ can reduce the strength.

3.1.2 Homogenization of specimens

In order to investigate the effect of PBHT on microstructure and mechanical properties of the joints, homogenization of the specimens was performed at 1000 °C for 1 h and 4 h. The aim of this PBHT was as follows:

- Achieving a more uniform microstructure
- Achieving a more uniform hardness profile across the joint
- Minimizing stress concentration
- Stress releasing

Figure 7 shows the effect of PBHT time (1 h and 4 h) on the microstructure of the joints brazed at 1050 °C (Fig. 7a, b) and 1170 °C (Fig. 7c, d). The thickness of ASZ increased with increasing PBHT time for the joint made at the brazing temperature of 1050 °C, and decreased with the increase of PBHT time for the joint made at the brazing temperature of 1170 °C. This is because diffusion is a thermally activated process and MPD atoms (boron and silicon) diffused insufficiently from liquid filler to solid base metal in the specimen brazed at a relatively low temperature of 1050 °C. As a result, regarding Fig. 7a and b with increasing PBHT time from 1 to 4 h, the ASZ width increased from 290 to 340 µm, respectively. In the case of the joint made at higher brazing temperature, the diffusion rate of MPD atoms into the base metal was higher during brazing. As a result, regarding Fig. 7c and d with increasing PBHT time from 1 to 4 h, the ASZ width decreased from 630 to 540 µm, respectively. This is because, in longer PBHT times, a higher number of MPD atoms have the opportunity to diffuse out of the interlayer. Therefore, by increasing the bonding time, the isothermal solidification front can progress further toward the centerline, and this fact will disturb ASZ formation.

Another interesting matter about Fig. 7d is the dissolution of intermetallic phases and more uniform microstructure in comparison with the microstructure in Fig. 7c. This issue

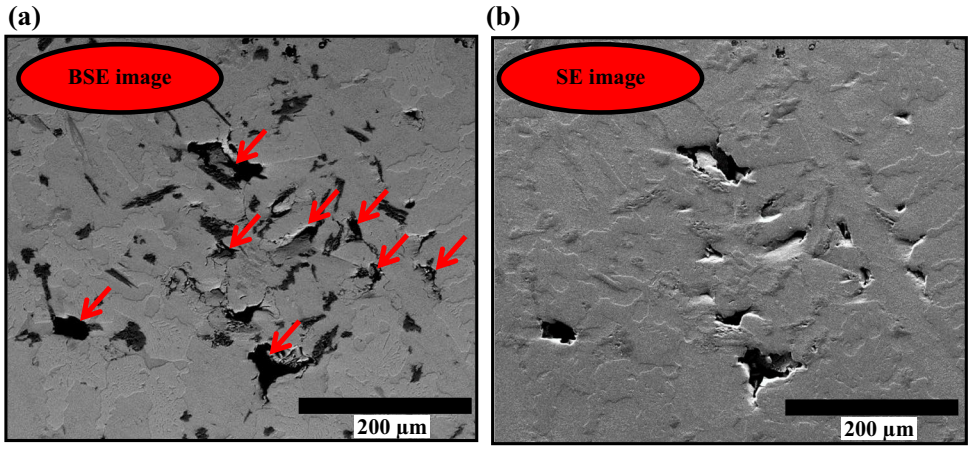

Fig. 6 Void-like defects observed in the SEM micrograph of the ASZ for the sample brazed at a bonding temperature of 1170 °C, **a** BSE image and **b** SE image

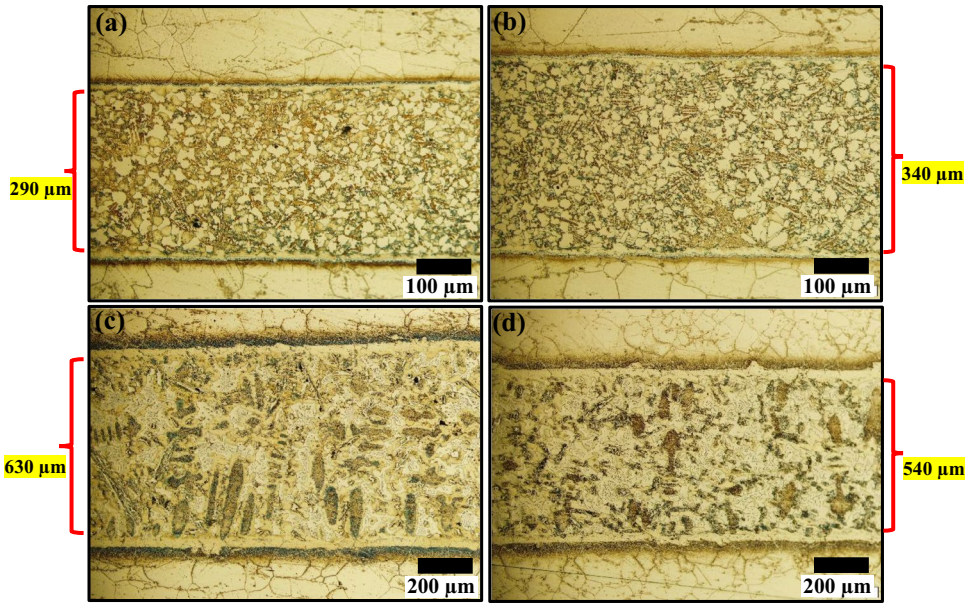

Fig. 7 The effect of PBHT at 1000 °C, on the microstructure of the joints **a** brazed at 1050 °C and homogenized for 1 h, **b** brazed at 1050 °C and homogenized for 4 h, **c** brazed at 1170 °C and homogenized for 1 h, and **d** brazed at 1170 °C and homogenized for 4 h

is better observed in Fig. 8 which indicates the EDS line scan of elements across the red dashed line for joint made at 1170 °C and homogenized at 1000 °C for 4 h. The variation of Ni, Cr, Mo, and MPD elements across the interface is continuous and smooth compared to the as-brazed specimen (Fig. 4). Additionally, the absence of intermetallic compounds in the diffusion zone is deduced by the smoothly varying nature of the profile curves. This indicates that PBHT leads to a more homogenous interface region via the dissolution of intermetallic phases. This is because the brazing process is a diffusion control phenomenon [27].

3.2 Mechanical properties of the joints

3.2.1 Microhardness

Figure 9 exhibits the variation of microhardness in the joint region as a function of distance from the center of interface for joints created at brazing temperatures of 1050 °C (stretch line curves) and 1170 °C (dashed line curves) with different PBHT times of 0, 1, and 4 h. It can be seen that substantial changes can be observed at the joint interface, which is directly related to the composition and thickness of DAZ, ISZ, and ASZ generated. Fairly high hardness values (866 and 770 VHN for the specimens created at brazing temperatures of 1050 and 1170 °C, respectively) are observed in the ASZ of specimens that were not undergone PBHT. These values are much greater than those for the NIMONIC 105 base metal. Khakian et al. [6] have reported that intermetallic phases that form during non-isothermal solidification possess very high hardness (750HVN). These brittle phases are suitable sites for crack initiation and therefore reduce the mechanical properties of the joint. These high hardness values are not seen in the joint region of the specimens that have undergone PBHT. This approves that PBHT leads to a more homogenous interface region via the dissolution of intermetallic phases. Figure 9 indicates that PBHT resulted in more uniform hardness profiles across the joint

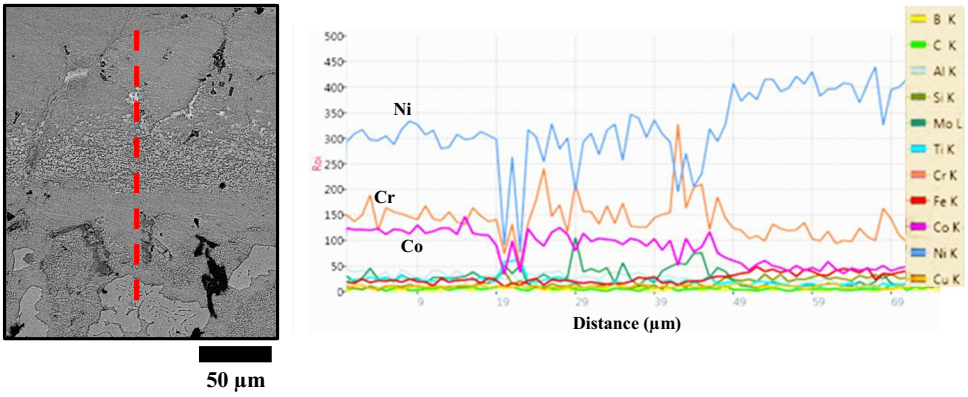

Fig. 8 BSE micrograph of the interface and respective EDS line scan of elements across the red dashed line for joint made at 1170 °C and homogenized at 1000 °C for 4 h

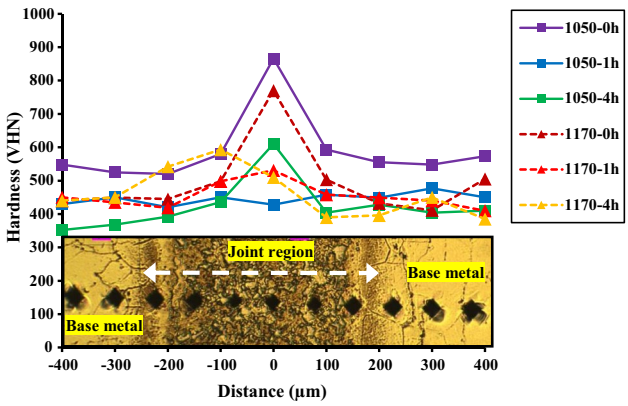

Fig. 9 Microhardness profiles across the joint region as a function of distance from the center of interface for joints created at brazing temperatures of 1050 °C (stretch line curves) and 1170 °C (dashed line curves) with different PBHT times of 0, 1, and 4 h

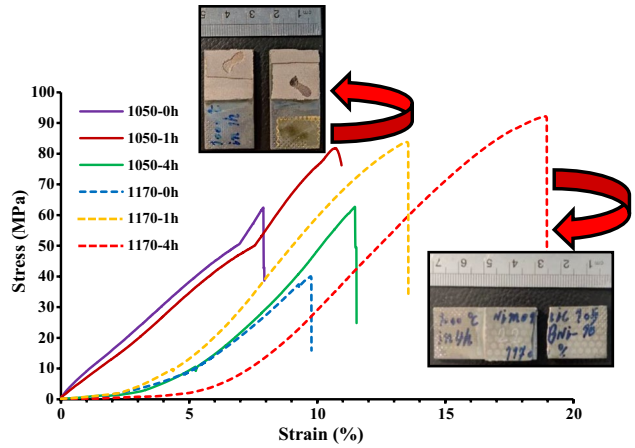

Fig. 10 Stress–strain curves obtained by a room-temperature shear strength test of the brazed joints with respect to different brazing temperatures and PBHT times discussed in this study

that, in turn, led to less stress concentration. Remarkably, the hardness between 450 and 550 HVN tended to correspond with indents on the eutectic constituent and matrix. The high hardness of about 800 HVN suggests the probability for the precipitation of Cr-rich intermetallics discussed in Fig. 5. Aside from these two observations, little difference in the hardness values at different brazing temperatures was noticed indicating brazing temperature did not have much effect on hardness. Instead, PBHT time has a considerable effect on phase formation and distribution. Thus, the microstructure and microhardness are consistent with the formation of brittle intermetallic compounds in ASZ. To minimize the extent of these detrimental phases, it is necessary to perform PBHT. On the other hand, Fig. 9 indicates that PBHT lowers the base metal hardness because of grain growth, which, in turn, can deteriorate the mechanical properties of the base metal.

3.2.2 Shear strength

The shear strength of the brazed specimens was determined by the single lap shear test. An illustration of the joint geometry prepared for performing the shear strength tests is shown in Fig. 1. Figure 10 shows room-temperature shear strength test results of the brazed joints with respect to different brazing temperatures and PBHT times discussed in this study. The strength of all joints is lower than that of NIMONIC 105 base material, and in all samples, failure occurred across the bonded interface except one. From Fig. 10, it can be seen that the highest shear strength of the brazed joint made at 1170 °C followed by 4-h PBHT at 1000 °C case can be up to 92.2 MPa. The ductility of this specimen was as high as 19.0%, which is approximately 75% of the ductility of NIMONIC 105. This sample failed away from the base metal, as seen in Fig. 10. The maximum ductility recorded in the present study is higher than those obtained in all similar previous works with different variables [3–6, 10, 27].

It is obvious that the shear strength of brazed joints is directly associated with that of joint microstructure. According to the literature [27–29], the shear strength and ductility of brazed joints depend on different complicated factors that are summarized in the following:

- Both the quantity and the distribution of intermetallic compounds in the joint region

As shown in Fig. 3, brazing temperature increment will increase the width of DAZ (quantity of precipitates) and change the morphology of precipitates, thus decreasing the shear strength of brazed joints from 62.4 to 40 MPa. The shear strength of joints made at a brazing temperature of 1170 °C remarkably increased from 40 to 83.8 MPa and finally reached the maximum value of 92.2 MPa via PBHT. This is because PBHT resulted in the formation of a more uniform microstructure and distribution of intermetallic compounds in the joint region. With extending PBHT time, the elements diffused deep into the substrates and gradually became uniform. Thus, the number of brittle intermetallic compounds decreased, and the corresponding shear strength increased. Moreover, according to Zhang et al. [29], the ductility of the brazed joints depended on the quantity of the boride precipitation in the DAZ, largely. High ductility of homogenized joints made at a brazing temperature of 1170 °C (13.5% and 19.0% for PBHT time of 1h and 4h, respectively) can be attributed to further diffusion of MPDs and intermetallic dissolution. In other words, it can be said that large stress concentration caused by borides was relieved during PBHT.

- The base metal grain growth

This factor was significant when the brazing temperature was 1170°C (Fig. 2b). The higher brazing temperature deteriorated the performance of base metal, resulting in the decrease of shear strength of the brazed joint to 40 MPa. On the other hand, in the case of the joint made at a brazing temperature of 1050 °C, a higher PBHT time of 4h led to lower shear strength (62.7 MPa) in comparison with a lower PBHT time of 1h (81.8 MPa). This finding can be attributed to the same factor.

- ASZ thickness

As mentioned earlier, the phases formed in the centerline eutectic (ASZ) are deleterious to the mechanical properties. The centerline eutectic phases are avoided by completing isothermal solidification. However, if isothermal solidification is incomplete, the microstructure can be improved with a diffusion heat treatment [17]. It is evident that for the joint made at brazing temperature of 1050 °C, homogenization of the specimen for 1h can increase the shear strength from 62.4 to 81.8 MPa. This is in accordance with the study of Khakian et al. [6] that there is a reverse relationship between bonding strength and ASZ thickness. As it is shown in Fig. 2a and Fig. 7a, PBHT at 1000 °C will extenuate the ASZ width from 470 to 290 µm. As the same way, regarding Fig. 7a and b with increasing PBHT time from 1 to 4h, the ASZ width increased from 290 to 340 µm. As a result, the shear strength of the joint decreased to 62.67 MPa for higher PBHT time of 4h.

- Brazing time and temperature

Kim et al. [10] found that increasing the brazing temperature increased the wettability of the filler metal and, therefore, the fracture strength increased. However, in the present study, increasing the brazing temperature from 1050 to 1170 °C resulted in a shear strength decline from 62.7 to 40.0 MPa. It can be concluded that blindly increasing the brazing temperature will not improve the joint performance. However, it will increase the possibility of defects (the voids observed in Fig. 6). Another mechanism that improves fracture strength is the diffusion of solid solution strengthening elements such as chromium, cobalt, aluminum, and titanium that diffused from the filler metal powder into the joint. Thus, by increasing the PBHT time (from 0 to 4h), the shear strength of joints made at brazing temperature of 1170 °C remarkably increased from 40 to 83.8 MPa and finally reached the maximum value of 92.2 MPa, because the microstructure becomes more homogeneous.

- Voids

Drastic decrease in the shear strength of a joint made at the brazing temperature of 1170 °C can be attributed to the voids observed in Fig. 6. Voids are significant stress concentration sites and have a detrimental influence on the mechanical properties of the joints. As a result, the corresponding shear strength of the joint was drastically reduced to 40.0 MPa.

3.3 Cyclic oxidation results

In order to investigate the high-temperature performance of the joints, cyclic oxidation test is performed to compare the oxidation resistance of the selected specimens. The mass change with the number of oxidation test cycle curves corresponds to the selected brazements created at brazing temperature of 1170 °C with PBHT times of 0 and 4 h, during cyclic oxidation at 1100 °C in air which is shown in Fig. 11. In fact, the spalling rate is a measure to compare oxidation resistance in cyclic conditions [30]. The results show that the weight changes include an increase in the weight of the sample during the initial cycles (up to the 15th cycle) and then a decrease in the weight of the sample. As mentioned previously, the formation of Cr-rich and Mo-rich intermetallic compounds during the brazing process leads to the discharge of these elements from the center line of the brazements. These brittle phases would have a detrimental effect on the high-temperature performance of the alloy and make it prone to selective corrosion or oxidation. This finding is in good agreement with other investigations [3, 6, 9]. As mentioned, performing PBHT will result in a more uniform distribution of Ni, Cr, Mo, and MPD elements across the interface (Fig. 8) and, in turn, increases the resistance to oxidation. Thus, the homogeneous distribution of Mo and Cr

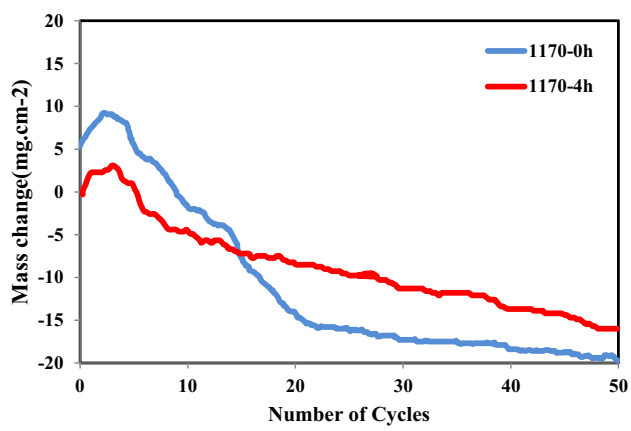

Fig. 11 Mass change curves of selected brazements created at brazing temperatures of 1170 °C with PBHT times of 0 and 4 h during cyclic oxidation at 1100 °C in air

in the joint region seems to be a crucial factor about oxidation resistance improvement.

4 Conclusions

The innovative approach of NIMONIC 105 brazing using BNi-2 filler, followed by PBHT, was experimentally investigated in this paper. Considering the results achieved, the following conclusions can be drawn:

1. The DAZ consists of globular/cuboidal and needle-like precipitates distributed in the interface. The precipitates in the DAZ were mainly composed of Ni–Cr-Mo-rich borides. The morphology and distribution of these secondary phases depend on the brazing temperature. So, the brazing temperature increment will increase the width of this DAZ from 12 to 35 µm.
2. The ISZ was a precipitation-free zone, mainly consisting of gamma solid solution. With the rise of brazing temperature from 1050 to 1170 °C, the thicknesses of ISZ increase significantly from 15 to 30 µm, respectively. The reason is that the rate of MPD diffusion into base metal is higher at a higher temperature.
3. Brazing time of 8 min employed in this study was insufficient to complete the isothermal solidification process. As a result, the remained liquid undergoes super cooling and ASZ with eutectic microstructure that contains fine precipitates formed. ASZ contains the matrix solid solution of gamma-nickel, Ni-rich boride, and two Cr-rich phases. Cr-rich boride and Cr-rich intermetallic compounds are detrimental phases that formed in this zone. Void formation in ASZ reduced the strength significantly.
4. Homogenization of the brazements was performed at 1000 °C for 1 h and 4 h in order to achieve a more uniform microstructure. PBHT led to a more uniform hardness profile across the joint and a more homogenous interface region via the dissolution of intermetallic phases. PBHT time had a dual effect on the thickness of ASZ. So, the thickness of ASZ increased with increasing PBHT time for the joint made at the brazing temperature of 1050 °C and decreased with the increase of PBHT time for the joint made at the brazing temperature of 1170 °C.
5. The shear strength of joints made at a brazing temperature of 1170 °C remarkably increased from 40 to 83.8 MPa and finally reached the maximum value of 92.2 MPa via PBHT. This is because PBHT resulted in the formation of a more uniform microstructure and distribution of intermetallic compounds in the joint region.
6. Performing PBHT will result in a more uniform distribution of Ni, Cr, Mo, and MPD elements across the interface and, in turn, increases the resistance to oxidation. Thus, the homogeneous distribution of Mo and Cr in the joint region seems to be a crucial factor about oxidation resistance improvement.

5 Proposal for future work

The quality of the brazement needs to be improved by the further design of interlayer composition and further optimization of the bonding parameters. This will include the insertion of an interlayer containing a high amount of refractory elements such as tungsten that effectively retard atomic diffusion and control the formation of brittle boride precipitates. The authors intend to study this approach in subsequent studies.

The high-temperature performance of the repaired joints is another important issue. High-temperature tensile strength and stress-rupture life are suggested to be supplemented in future work.

Declarations

Conflict of interest The authors declare no competing interests.

References

1. Reed RC (2006) The superalloys - fundamentals and applications. Cambridge University Press, New York
2. Schwartz MM (2003) Brazing, 2nd edn. ASM International
3. Arhami F, Mirsalehi SE, Sadeghian A (2019) Effect of bonding time on microstructure and mechanical properties of diffusion brazed IN-939. J Materials Process Tech 265:219–229. https://doi.org/10.1016/j.jmatprotec.2018.10.021
4. Li W, Jin T, Sun X, Guo Y, Guan H, Hu Z (2003) Study of NieCreCoeWeMoeB interlayer alloy and its bonding behaviour for a Ni base single crystal superalloy. Scr Mater 48(9):1283–1288
5. Liu J, Jin T, Zhao N, Wang Z, Sun XF, Guan HR, Hu ZQ (2007) Effect of temperature on formation of borides in TLP joint of a kind of nickel base single crystal superalloy. Mater Sci Forum 546:1245–1248
6. Khakian M, Nategh S, Mirdamadi S (2015) Effect of bonding time on the microstructure and isothermal solidification completion during transient liquid phase bonding of dissimilar nickel-based superalloys IN738LC and NIMONIC 75. J Alloy Compd 653:386–394. https://doi.org/10.1016/j.jallcom.2015.09.044
7. Mofid MA, A (2021) Mahdavi Nejad, "Flame spray assisted TLP bonding of Ti alloy to Al alloy." Materials Chem Physics 263:124404
8. McGuire D, Huang X, Nagy D, Chen W (2010) Effect of tungsten addition on the nucleation of borides in wide gap brazed joint. J Eng Gas Turbines Power 132:062101–062111. https://doi.org/10.1115/1.4000136
9. Wu N, Li YJ, Ma QS (2014) Microstructure evolution and shear strength of vacuum brazed joint for super-Ni/NiCr laminated composite with Ni–Cr–Si–B amorphous interlayer. Mater Des 53:816–821. https://doi.org/10.1016/j.matdes.2013.07.063
10. Kim YH, Kim KT, Kim IH (2006) Effect of mixing ratio on mechanical properties of wide-gap brazed ni-based superalloy with NI-Si-B Alloy powder. Key Eng Mater 306–308:935–940

11. Hadibeyk S, Beidokhti B, Sajjadi SA (2018) The effect of interlayer thickness, bonding temperature and atmosphere on transient liquid phase bonding of GTD-111 to FSX-414. J Mater Process Technol 255:673–678. https://doi.org/10.1016/j.jmatprotec.2018.01.022
12. Arafin MA, Medraj M, Turner DP, Bocher P (2007) Effect of alloying elements on the isothermal solidification during TLP bonding of SS 410 and SS 321 using a BNi-2 interlayer. Mater Chem Phys 106(1):109–119
13. Ruiz-Vargas J, Siredey-Schwaller N, Gey N, Bocher P, Hazotte A (2013) Microstructure development during isothermal brazing of Ni/BNi-2 couples. J Mater Process Technol. 213(1):20–29
14. Liu D, Song Y, Shi B, Zhang Q, Song X, Niu H, Feng J (2018) Vacuum brazing of GH99 superalloy using graphene reinforced BNi-2 composite filler. J Mater Sci Technol 34(10):1843–1850. https://doi.org/10.1016/j.jmst.2018.02.008
15. HM. Hdz-García, AI. Martinez, R. Mu˜noz-Arroyo, JL. Acevedo-Dávila, F.García-Vázquez, FA. Reyes-Valdes, Mater. Sci Technol 2014 30 259–262
16. Shen J, Liu YC, Han YJ, Tian YM, Gao HX (2006) J Electron Mater 35:1672–1679
17. Duvall DS, Owczarski WA, Paulonis DF (1973) TLP bonding--a new method. Welding Journal, Chicago 203–214
18. Pouranvari M, Ekrami A, Kokabi A (2013) Phase transformations during diffusion brazing of IN718/Ni-Cr-B/IN718. Mater Sci Technol 29(8):980–984
19. COTEST (n.d.) Development of a code practice for the characterization of high temperature materials performance, 5th EU Framework program G6RD-CT-2001- 00639(2004)
20. Naeimian H, Mofid MA (2020) Effect of joining temperature on Al2024/Ag/Ti-6Al-4V joints during TLP bonding. Int J Mater Res (formerly Z Metallkd) 111(5):424–431. https://doi.org/10.3139/146.111902
21. Naeimian H, Mofid MA (2020) Study of TLP bonding of Ti-6Al-4V to Al2024 using thermal spray Babbitt alloy interlayer. Trans Nonferrous Met Soc China 30:1267–1276. https://doi.org/10.1016/S1003-6326(20)65294-3
22. Mofid MA, Loryaei E (2019) Investigating microstructural evolution at the interface of friction stir weld and diffusion bond of Al and Mg alloys. J Materials Res Technol 8(5):3872–3877
23. Gale W, Butts D (2004) Transient liquid phase bonding. Sci Technol Weld Join 9(4):283–300
24. Gale W, Wallach E (1991) Microstructural development in transient liquid phase bonding. Metall Trans 22(10):2451–2457
25. Alloy Phase Diagrams ASM Handbook, tenth ed 3 1992 2.83–2.92
26. Sung P, Poirier D (1999) Liquid solid partition ratios in nickel base alloys. Metall Mate Trans 30(8):2173–2181
27. Xu Y, Qiu X, Wang S, Luo C, Lu Y, Xing F (2021) Interfacial microstructure and mechanical properties of tungsten based powder alloy and superalloy GH907 diffusion brazing joint with Cu-Ni-V-Ti interlayer. Vacuum 184:109793. https://doi.org/10.1016/j.vacuum.2020.109793
28. Hoppin BYGS, Berry TF (1970) Activated diffusion bonding a new joining process produces high strength joints. Weld Res Suppl. 90:505–509
29. Zhang LX, Sun Z, Xue Q, Lei M, Tian XY (2016) Mater Des 90:949–957
30. Evans AG, Clarke DR, Levi CG (2008) The influence of oxides on the performance of advanced gas turbines. J Eur Ceram Soc 28:1405–1419

Publisher's note Springer Nature remains neutral with regard to jurisdictional claims in published maps and institutional affiliations.

Springer Nature or its licensor (e.g. a society or other partner) holds exclusive rights to this article under a publishing agreement with the author(s) or other rightsholder(s); author self-archiving of the accepted manuscript version of this article is solely governed by the terms of such publishing agreement and applicable law.